Journal of Structural Biology 174 (2011) 252–257

Contents lists available at ScienceDirect

Journal of Structural Biology

journal homepage: www.elsevier.com/locate/yjsbi

Structure Report

Crystal structure of the mucin-binding domain of Spr1345 from *Streptococcus pneumoniae*

Yang Du [a,1], Yong-Xing He [a,1], Zhen-Yi Zhang [a], Yi-Hu Yang [a], Wei-Wei Shi [a], Cécile Frolet [b,c,d], Anne-Marie Di Guilmi [b,c,d], Thierry Vernet [b,c,d], Cong-Zhao Zhou [a], Yuxing Chen [a,*]

[a] School of Life Sciences, University of Science and Technology of China, Hefei, Anhui 230026, PR China
[b] CEA, Institut de Biologie Structurale Jean-Pierre Ebel, Grenoble, France
[c] CNRS, Institut de Biologie Structurale Jean-Pierre Ebel, Grenoble, France
[d] Université Joseph Fourier, Institut de Biologie Structurale Jean-Pierre Ebel, Grenoble, France

ARTICLE INFO

Article history:
Received 11 September 2010
Received in revised form 22 October 2010
Accepted 29 October 2010
Available online 3 November 2010

Keyword:
Mucin-binding protein
Mucin-binding domain
Crystal structure
Adhesin
Streptococcus pneumoniae

ABSTRACT

The surface protein Spr1345 from *Streptococcus pneumoniae* R6 is a 22-kDa mucin-binding protein (MucBP) involved in adherence and colonization of the human lung and respiratory tract. It is composed of a mucin-binding domain (MucBD) and a proline-rich domain (PRD) followed by an LPxTG motif, which is recognized and cleaved by sortase, resulting in a mature form of 171 residues (MF171) that is anchored to the cell wall. We found that the MucBD alone possesses comparable *in vitro* mucin-binding affinity to the mature form, and can be specifically enriched at the surface of human lung carcinoma A549 cells. Using single-wavelength anomalous dispersion (SAD) phasing method with the iodine signals, we solved the crystal structure of the MucBD at 2.0 Å resolution, the first structure of MucBDs from pathogenic bacteria. The overall structure adopts an immunoglobulin-like fold with an elongated rod-like shape, composed of six anti-parallel β-strands and a long loop. Structural comparison suggested that the conserved C-terminal moiety may participate in the recognition of mucins. These findings provided structural insights into host-pathogen interaction mediated by mucins, which might be useful for designing novel vaccines and antibiotic drugs against human diseases caused by pneumococci.

1. Introduction

The Gram-positive bacterium *Streptococcus pneumoniae* (also referred to as pneumococcus) is one of the most notorious human pathogens, and is responsible for many community-acquired diseases. It claims over 1.5 million lives worldwide per year, especially in young children and the elderly (Bogaert et al., 2004; Kadioglu et al., 2008). Usually, the pneumococci commensally reside in the nasopharyngeal cavity and on the mucosal surface of the upper airway without causing symptoms. Upon appropriate occasions like concurrent respiratory viral infection, they initiate rapid inflammatory responses, which lead to acute local infections and serious human diseases such as otitis, pneumonia, septicemia and meningitis (Bergmann and Hammerschmidt, 2006). The pathogenesis of pneumococcal infection begins with the adherence to the host epithelial cells, which is mediated by a diverse group of bacterial surface proteins including choline-binding proteins, lipoproteins, some surface-associated enzymes, and proteins with an LPxTG motif (Bergmann and Hammerschmidt, 2006; Bogaert et al., 2004; Regev-Yochay et al., 2004). These proteins can bind to a variety of host receptors and may be involved in adhesion to extracellular matrix components, and/or evasion of host immunologic clearance (Frolet et al., 2010; Kadioglu et al., 2008). Many efforts have focused on characterization of these surface-exposed adherence proteins, which could be helpful in designing more effective protein-based vaccines (Bergmann and Hammerschmidt, 2006; Bogaert et al., 2004; Nobbs, 2009).

The mucin-binding proteins (MucBP) are a group of surface proteins that facilitate adhesion of pathogens to the host via interactions with the mucus secreted by epithelial cells. The major constituents of the mucus are mucins, a family of high molecular weight, heavily O-linked glycosylated proteins. The surface protein Mub from *Lactobacillus reuteri* was identified as a high molecular weight MucBP with 14 repeats of the mucin-binding domain (MucBD) (MacKenzie et al., 2009; Roos and Jonsson, 2002). In contrast, Spr1345 from *S. pneumoniae* R6 is a low molecular weight

Abbreviations: MucBP, mucin-binding protein; MucBD, mucin-binding domain; PRD, proline-rich domain; ELISA, enzyme-linked immunosorbent assay; BSA, bovine serum albumin; RT, room temperature; SAD, single-wavelength anomalous dispersion; FITC, fluorescein isothiocyanate; PDB, protein data bank.

* Corresponding author. Fax: +86 0551 3600406.
E-mail address: cyxing@ustc.edu.cn (Y. Chen).

[1] Authors contributed equally to this work.

1047-8477/$ - see front matter © 2010 Elsevier Inc. All rights reserved.
doi:10.1016/j.jsb.2010.10.016

MucBP with a single MucBD. In addition to the MucBD, Spr1345 has a proline-rich domain (PRD) followed by an LPxTG motif, which is recognized and cleaved by sortase between the Thr and Gly residues, resulting in the mature form protein of 171 residues (MF171) anchored to the cell wall (Fig. 1A).

Here, we report the crystal structure of the MucBD of Spr1345 at 2.0 Å resolution, representing the first MucBD structure from pathogenic bacteria. The overall structure adopts an immunoglobulin-like β-sandwich fold of an elongated rod-like shape composed of six anti-parallel β-strands and a long loop. Comparative structural analysis revealed a conserved C-terminal moiety, which is crucial for the recognition of protein partners such as mucin. The structural and biochemical analysis of Spr1345 might help design novel vaccines to fight against the pneumococcal infections.

2. Cloning, expression, and purification of the MucBD of Spr1345

The full-length Spr1345 is subject to degradation upon expression and purification, so we subcloned two truncated versions: the predicted MucBD (residues 1–104) and MF171 (residues 1–171). A hexa-histidine (6 × His) tag was added to the N-terminus of each recombinant protein before overexpression in *Escherichia coli* Bl21-RIL (DE3) strain (Novagen, Madison, USA) in 2 × YT culture medium (16 g tryptone, 10 g yeast extract, and 5 g NaCl per liter). Cells were grown at 37 °C to an $A_{600\ nm}$ of 0.6. Expression of recombinant proteins was induced with 0.2 mM isopropyl-β-D-thiogalactoside and cell growth was continued for 20 h at 16 °C before harvesting. Cells were collected by centrifugation at 4000 × *g* for 20 min and resuspended in lysis buffer (20 mM Tris–Cl, pH 8.0, 150 mM NaCl). After 5 min of sonication and centrifugation at 12,000 × *g* for 25 min, the supernatant containing the soluble target protein was collected and loaded onto a Ni–NTA column (GE Healthcare) equilibrated with binding buffer (20 mM Tris–Cl, pH8.0, 150 mM NaCl). Target proteins was eluted with 200 mM imidazole, and further loaded onto a Superdex 75 column (GE Healthcare) equilibrated with 20 mM Tris–Cl, pH 8.0, 150 mM NaCl. Fractions containing the target protein were collected and concentrated to 20 mg/ml. Protein purity was evaluated by SDS–PAGE and samples were stored at −80 °C.

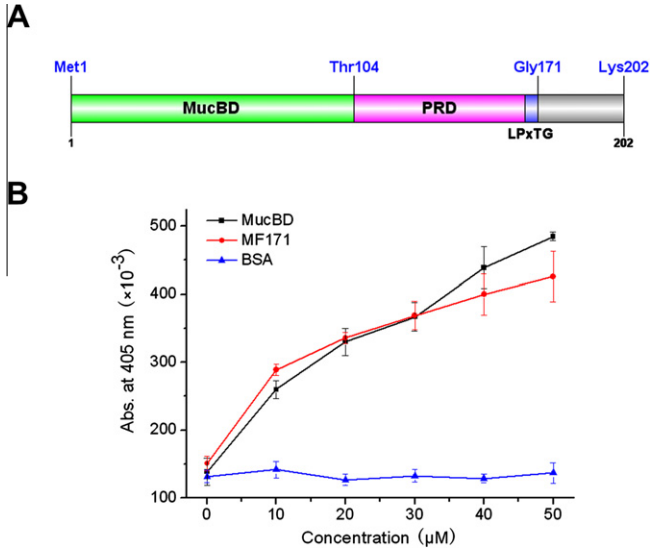

Fig.1. Definition of the MucBD of Spr1345. (A) Organization of Spr1345. The domain organization was drawn with Domain Graph, version 1.0 (Ren et al., 2009). (B) Mucin-binding affinity assays. The increase in absorbance at 405 nm (Y) was plotted against the protein concentration (X). BSA was used as a negative control. MucBD, black; MF171, red; BSA, blue. (For interpretation of the references in color in this figure legend, the reader is referred to the web version of this article.)

Table 1
Crystal parameters, data collection and structure refinement.

Data processing	
Space group	$I4_122$
Unit cell parameters *a*, *b*, *c* (Å)	73.16, 73.16, 108.81
α, β, γ (°)	90, 90, 90
Resolution range (Å) overall/outer shell[a]	37.48–2.00 (2.11–2.00)
Unique reflections	10,342
Completeness (%)	100.0 (100.0)
$\langle I/\sigma(I)\rangle$	29.2 (10.4)
R_{merge}[b] (%)	5.0 (19.9)
Redundancy	8.4 (8.3)
Refinement statistics	
Resolution range (Å)	25.87–2.00
R-factor[c]/R-free[d] (%)	21.3/26.4
Number of water atoms	150
RMSD[e] bond length (Å)	0.007
RMSD bond angles (°)	1.014
Average of B-factors (Å^2)	26.2
Ramachandran plot[f]	
Most favored (%)	99.0
Additional allowed (%)	1.0
Outliers (%)	0

[a] The values in parentheses refer to statistics in the highest bin.
[b] $R_{merge} = \sum_{hkl}\sum_i|I_i(hkl) - \langle I(hkl)\rangle|/\sum_{hkl}\sum I_{ii}(hkl)$, where $I_i(hkl)$ is the intensity of an observation and $\langle I(hkl)\rangle$ is the mean value for its unique reflection; Summations are over all reflections.
[c] R-factor = $\sum_h|Fo(h) - Fc(h)|/\sum_h Fo(h)$, where Fo and Fc are the observed and calculated structure-factor amplitudes, respectively.
[d] R-free was calculated with 5% of the data excluded from the refinement.
[e] Root-mean square-deviation from ideal values.
[f] Categories were defined by Molprobity.

3. Crystallization, data collection and structure determination

Crystals of the Spr1345 MucBD were grown at 289 K through hanging drop vapor-diffusion techniques by mixing 1 μL of 20 mg/mL protein sample with an equal volume of reservoir solution (22% polyethylene glycol 4000, 0.1 M Tris–HCl pH 8.5, 0.2 M Li_2SO_4). Crystals appeared in 2 weeks. Before data collection, crystals were soaked in cryoprotectant solution (reservoir solution supplemented with 25% glycerol) containing 1 M potassium iodine for ~20 s. Diffraction images were collected at 100 K in a liquid nitrogen stream using a Rigaku MM007 X-ray generator (λ = 1.5418 Å) with a MarRearch 345 image-plate detector (USTC, Hefei, China). Data were processed with MOSFLM 7.0.4 (Leslie, 1992) and scaled with SCALA (Evans, 1993). The structure was determined by the SAD phasing technique with iodine anomalous signal using the program SHELX C/D/E (Sheldrick, 2008). The initial model was refined using the maximum likelihood method implemented in REFMAC5 (Murshudov et al., 1997) as part of the CCP4 program suite and rebuilt interactively using σ_A-weighted electron density maps with coefficients 2*mFo-DFc* and *mFo-DFc* in the program COOT (Emsley and Cowtan, 2004). During the later stages, restrained positional and B-factor refinement was performed using the program phenix.refine. Refinement converged to an R-factor of 21.3% and R-free of 26.4%. The final models were evaluated with the programs MOLPROBITY (Davis et al., 2007) and PROCHECK (Laskowski et al., 1993). Data collection and structure refinement statistics are in Table 1. All structure figures were prepared with the program PyMOL (DeLano, 2002).

4. Enzyme-linked immunosorbent assays (ELISA) and immunofluorescence microscopy

Mucin from porcine stomach (type III, Sigma–Aldrich) was dissolved in phosphate-buffered saline (PBS) at a concentration of 160 μg/mL, and immobilized on a 96-well microplate (BBI, Canada) at 100 μL of mucin per well by incubating overnight at 4 °C. Bovine serum albumin (BSA) was used as a negative control. Wells were

blocked with 100 μL/well of 1% BSA for 2 h at room temperature (RT), and washed with 200 μL/well PBS-0.05% Tween-20 (PBST) for three times before adding 50 μL of MucBD, MF171 and BSA each at five different concentrations in PBS, and incubating for 6 h at RT. Wells were washed and incubated with mouse monoclonal His-tag antibody (Cell Signaling Technology), diluted 1/1000 in PBST, overnight at 4 °C. After washing, wells were incubated with rabbit anti-mouse polyclonal antibody-alkaline phosphatase conjugate (Promega), diluted 1/2000 in PBST, for 1 h at RT, washed and developed with pNPP (Sangon) as substrate. Finally, the plate was measured at $A_{405\ nm}$ using a plate reader (BioTek). All data are the average of three independent experiments.

Fluorescein isothiocyanate (FITC) labeling of the MucBD and BSA was as described previously (Logue et al., 2009). Human lung epithelial carcinoma A549 cells were grown in Dulbecco's modified Eagle's medium supplemented with 10% fetal bovine serum, 100 units/mL penicillin, 100 μg/mL streptomycin and incubated in a humidified 5% CO_2 atmosphere at 37 °C until confluent monolayer established. For immunofluorescence studies, A549 cells were re-seeded and maintained overnight in Lab-Tek confocal chamber glass slides (Nunc). Cells were washed 3 times for 5 min each with PBS and fixed in 3.5% formaldehyde at RT for 5 min. After washing 3 times with PBS, cells were blocked with 5% BSA in PBS for 2 h at 4 °C and washed 3 times with PBS. Cells were incubated with 20 μM purified FITC-labeled MucBD while FITC-labeled BSA was used as the negative control (200 μL/well) for 1 h at RT. After staining, cells incubated were washed 3 times with PBS and mounted on a Zeiss LSM 510 confocal laser scanning microscope.

5. Mucin-binding of Spr1345 subdomains and adhesion to human lung epithelial cells

Unlike the full-length Spr1345, the two truncated proteins MucBD and MF171 were stable during purification. To evaluate whether the PRD contributes to the mucin-binding activity, ELISA was used to detect the interaction of the MucBD and MF171 with mucins. The interactions of both proteins with mucin were concentration-dependent, and both showed approximately the same binding pattern, implying that MucBD (Met1-Thr104) is a functionally sufficient unit for mucin binding (Fig. 1B).

To further determine whether the MucBD is an adhesion molecule, we performed an adhesion assay with human lung carcinoma A549 cells that express mucins (Berger et al., 1999). FITC-labeled MucBD proteins were found to be enriched at the surface of A549 cells, while no significant binding was observed for FITC-labeled BSA, which showed weak fluorescence intensity (Fig. 2). This indicated that the MucBD of Spr1345 was indeed an adhesin that interacted directly with the epithelial cells.

6. Overall structure of the MucBD of Spr1345

To better understand the structural basis of mucin-binding capacity, both the MucBD and MF171 were used for crystallization screening. Both drops of MucBD and MF171 produced crystals of MucBD that diffracted to 2.0 Å resolution. It belongs to the space group of $I4_122$, with one molecule in an asymmetric unit. The final model comprises residues Thr5-Ser104. The overall structure exhibits an elongated rod-like shape of approximately $15 \times 15 \times 80$ Å (Fig. 3A) that belongs to the immunoglobulin-like β-sandwich fold, consisting of six anti-parallel β-strands that form two β-sheets: one of four strands (β1-3 and 6) and the other of two strands (β4 and 5). Strands β1 and β2, containing 14 and 18 residues, respectively, are much longer than the rest, while strands β4 and β5 are only 3 residues long connected by a long loop of 22 residues (loopL). Within the β-sandwich and loopL, a large number of hydrophobic residues are buried such as Ile18, Val29, Val37, Trp62, Val65, Ile70, Tyr73 and Ile95, leading to the formation of a compact hydrophobic core. Sequence alignment of MucBDs

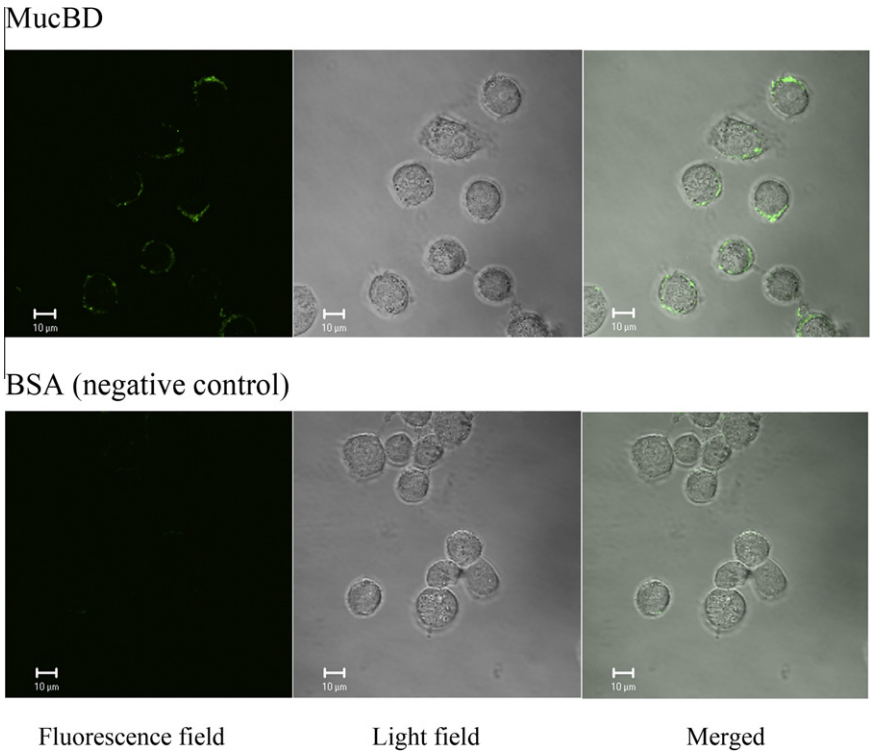

Fig.2. Binding of the Spr1345 MucBD to the surface of human lung epithelial A549 cells. The fluorescence field, light field and merged images are shown. FITC-labeled BSA was used as a negative control.

indicated that most of these hydrophobic residues are conserved, especially Trp62, Val65, Ile70 and Tyr73 in loopL, implying the indispensability of the hydrophobic core for structural stability (Fig. 4A).

7. Comparison with homologous structures

Using the Dali server (http://ekhidna.biocenter.helsinki.fi/dali_server/), we found that the MucBD resembles the C-terminal domain of the fifth repetitive MucBD (Mub-R5) from *L. reuteri* (PDB code 3I57, Z score 9.9, RMSD 2.8 Å over 95 Cα atoms, 28% sequence identity over 95 residues) and a putative adhesin from *Pediococcus pentosaceus* (PDB code 3LYY, Z score 9.8, RMSD 2.0 Å over 90 Cα atoms, 37% sequence identity over 90 residues) (Fig. 3B and C). Despite some variation in secondary structure elements, the three structures share a similar topology (Fig. 3D). The core structure of the MucBD is composed of a four-stranded β-sheet (β1-3 and β6), whereas that of the other two consists of two discrete β-sheets (β2′–β3′–β11′ and β1′–β4′–β5′ in Mub-R5; β1″–β2″–β9″ and β3″–β4″ in the putative adhesin). Besides, the MucBD has a much longer

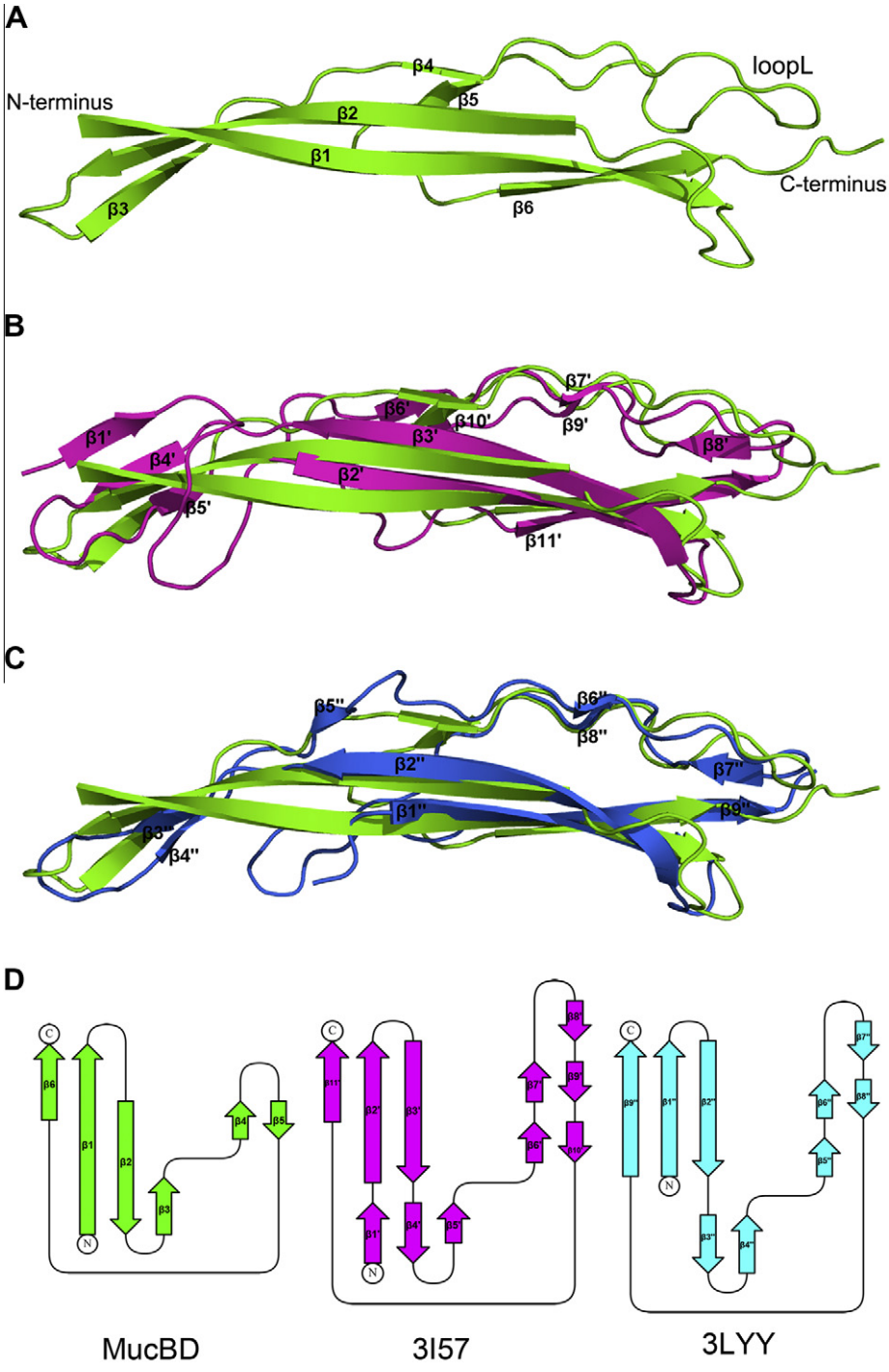

Fig.3. Comparative structural analysis of the Spr1345 MucBD. (A) Overall structure of the Spr1345 MucBD. Superposition of the Spr1345 MucBD against (B) the C-terminal domain of the Mub-R5 repeat from *L. reuteri* (magenta), and (C) a putative adhesin from *P. pentosaceus* (marine). Secondary structural elements of the latter two proteins are labeled β′ and β″, respectively. (D) Topology diagrams of the MucBD and two homologs. The β-strands are labeled sequentially.

β1-strand and loopL, a large part of which contributes to the hydrophobic core, and shows very few conformational displacements compared to that of Mub-R5 or the putative adhesin from *P. pentosaceus*. Structural and sequence alignment revealed a more conserved C-terminal moiety, implying that hot spots for recognizing protein partners are more likely to lie in this part of the MucBD.

8. Organizations of the MucBP family and implications from Spr1345

The MucBPs are found in a wide variety of bacterial surface proteins, most of which are from prokaryotes, especially the human-hosted bacteria such as pneumococci and lactobacilli through sequence analysis (http://www.ncbi.nlm.nih.gov/blast). We investigated all 62 subfamilies of MucBP in the Pfam database (Entry PF06458, http://pfam.sanger.ac.uk/), which show highly diversified organizations with varied numbers of MucBD, from single MucBD to 19 MucBDs. Seven representative homologs from other species were selected to exhibit the distinct organizations. These MucBPs share a C-terminal sorting signal LPxTG motif, but bear various copy numbers of MucBD (Fig. 4B). The various repeats of MucBD might have evolved via duplication, divergence and recombination for better colonization and survival in diverse environments of the host.

Notably, some MucBPs contain an additional PRD, which contains more than 30% of proline residues and usually adopts a

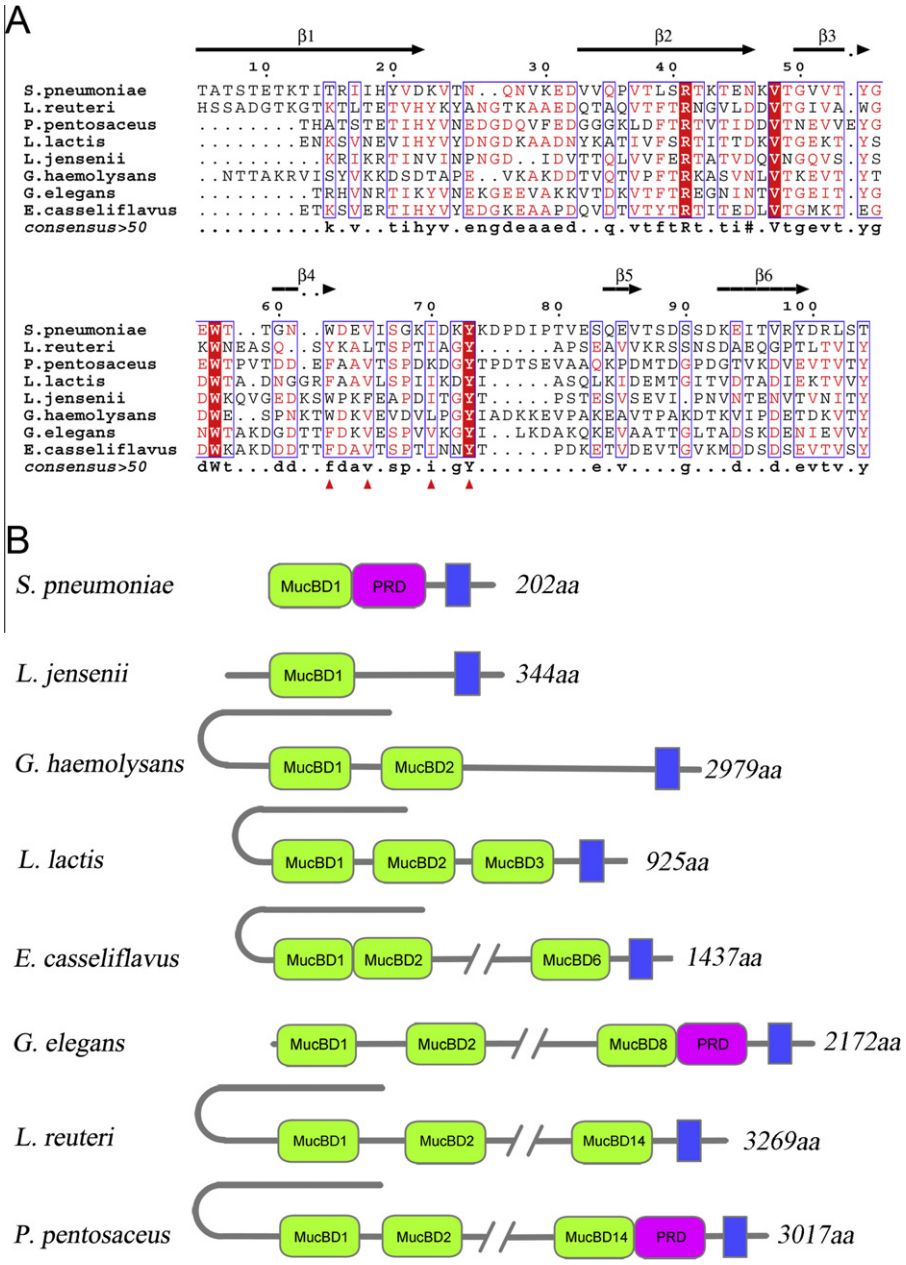

Fig.4. (A) Multiple sequence alignment of MucBDs from different species. Sequences are from *Streptococcus pneumoniae* (GenBank accession number: AAL00149), *Lactobacillus reuteri* (AAF25576, 28% sequence identity with the MucBD of Spr1345), *Pediococcus pentosaceus* (ABJ67225, 37%), *Lactococcus lactis* (CAL99029, 35%), *Lactobacillus jensenii* (EEI50617, 30%), *Gemella haemolysans* (EER67913, 22%), *Granulicatella elegans* (EEW92383, 32%), *Enterococcus casseliflavus* (EEV40788, 38%). Alignment was performed using MultAlin (Corpet, 1988) and ESPript (Gouet et al., 2003) (http://multalin.toulouse.inra.fr/multalin/). Conserved residues in loopL are marked with red triangles. (B) Diverse domain organizations of MucBPs. MucBD, chartreuse; PRD, magenta; LPxTG motif, blue. (For interpretation of the references in color in this figure legend, the reader is referred to the web version of this article.)

flexible left-handed polyproline II (PPII) helix conformation (Kay et al., 2000; Rucker et al., 2003; Williamson, 1994). Previously, in the cell surface adhesin antigen I/II from *Streptococcus mutans*, the PRD (92 residues) adopting elongated left-handed helical conformation was reported to aid in the protrusion of adhesin domains from the cell surface (Larson et al., 2010). Spr1345 possesses a 62-residue PRD, which did not contribute to mucin binding, as indicated by the comparable mucin-binding affinities of MucBD and MF171 (Fig. 1B). However, by adopting an elongated PPII helical conformation, the PRD might contribute to protrusion of the MucBD outwards from cell wall. Given that the 62-residue PRD of Spr1345 probably adopts a PPII helical conformation, it would extend the adhesive MucBD approximately 35 nm from the cell wall, which will facilitate the accessibility of MucBD to its protein partners.

The MucBD of Spr1345 was demonstrated to bind to three types of mucins with broad specificity and several polysaccharides such as hyaluronan, which suggests that Spr1345 interacts with carbohydrate moiety of mucins, regardless of specified mucin type (Bumbaca et al., 2007). Although certain residues such as the aromatic residues show a propensity to be in sugar-binding sites, the interactions between proteins with sugar chains of glycoproteins adopt diverse patterns (Taroni et al., 2000). The protein core of mucins is mainly covered with a polymeric sugar layer, which contains complicated and abundant sugar chains especially O-linked oligosaccharides. (Byrd and Bresalier, 2004). Therefore, these properties make it difficult for us to assign the mucin-binding site to a well-defined local region of the MucBD. However, a couple of relatively conserved surface residues, such as Val24, Asn61 and Tyr73, at the C-terminal moiety of the MucBD, might be involved in the recognition of sugars.

In summary, the low molecular weight MucBP Spr1345 from the surface of *S. pneumoniae* is implicated in adherence and colonization with host cells. Spr1345 has a single MucBD in contrast to the multiple MucBDs of its homologs with diverse organizations, especially those in the lactobacilli. This single MucBD possesses comparable mucin-binding affinity to the mature form. We determined the crystal structure of the MucBD, the first MucBD structure from pathogenic bacteria, at 2.0 Å resolution using an iodine-SAD technique. The structure bears structural similarity to the C-terminal domain of Mub-R5 repeat from *L. reuteri*, but represents a minimal mucin-binding unit. Since Spr1345 is one of the few pneumococcal adhesin molecules characterized to date (Bumbaca et al., 2007), our findings might provide insights into molecular function of Spr1345 for designing novel vaccines to fight against pneumococcal diseases.

9. Accession number

Coordinates and structural factors have been deposited in the Protein Data Bank under the accession code of 3NZ3.

Acknowledgments

This work was supported by the Ministry of Science and Technology of China (Grant No. 2009CB918804) and the National Natural Science Foundation of China (No. 30870488).

References

Berger, J.T., Voynow, J.A., Peters, K.W., Rose, M.C., 1999. Respiratory carcinoma cell lines. MUC genes and glycoconjugates. Am J Respir Cell Mol Biol 20, 500–510.
Bergmann, S., Hammerschmidt, S., 2006. Versatility of pneumococcal surface proteins. Microbiology 152, 295–303.
Bogaert, D., De Groot, R., Hermans, P.W., 2004. *Streptococcus pneumoniae* colonisation: the key to pneumococcal disease. Lancet Infect Dis 4, 144–154.
Bumbaca, D., Littlejohn, J.E., Nayakanti, H., Lucas, A.H., Rigden, D.J., Galperin, M.Y., Jedrzejas, M.J., 2007. Genome-based identification and characterization of a putative mucin-binding protein from the surface of *Streptococcus pneumoniae*. Proteins 66, 547–558.
Byrd, J.C., Bresalier, R.S., 2004. Mucins and mucin binding proteins in colorectal cancer. Cancer Metastasis Rev 23, 77–99.
Corpet, F., 1988. Multiple sequence alignment with hierarchical clustering. Nucleic Acids Res 16, 10881–10890.
Davis, I.W., Leaver-Fay, A., Chen, V.B., Block, J.N., Kapral, G.J., Wang, X., Murray, L.W., Arendall 3rd, W.B., Snoeyink, J., Richardson, J.S., Richardson, D.C., 2007. MolProbity: all-atom contacts and structure validation for proteins and nucleic acids. Nucleic Acids Res 35, W375–W383.
DeLano, W., 2002. The PyMOL Molecular Graphics System. DeLano Scientific, San Carlos, CA. http://www.pymol.org.
Emsley, P., Cowtan, K., 2004. Coot: model-building tools for molecular graphics. Acta Crystallogr D Biol Crystallogr 60, 2126–2132.
Frolet, C., Beniazza, M., Roux, L., Gallet, B., Noirclerc-Savoye, M., Vernet, T., Di Guilmi, A.M., 2010. New adhesin functions of surface-exposed pneumococcal proteins. BMC Microbiol 10, 190.
Gouet, P., Robert, X., Courcelle, E., 2003. ESPript/ENDscript: extracting and rendering sequence and 3D information from atomic structures of proteins. Nucleic Acids Res 31, 3320–3323.
Kadioglu, A., Weiser, J.N., Paton, J.C., Andrew, P.W., 2008. The role of *Streptococcus pneumoniae* virulence factors in host respiratory colonization and disease. Nat Rev Microbiol 6, 288–301.
Kay, B.K., Williamson, M.P., Sudol, M., 2000. The importance of being proline: the interaction of proline-rich motifs in signaling proteins with their cognate domains. FASEB J 14, 231–241.
Larson, M.R., Rajashankar, K.R., Patel, M.H., Robinette, R.A., Crowley, P.J., Michalek, S., Brady, L.J., Deivanayagam, C., 2010. Elongated fibrillar structure of a streptococcal adhesin assembled by the high-affinity association of alpha- and PPII-helices. Proc Natl Acad Sci USA 107, 5983–5988.
Laskowski, R.A., Moss, D.S., Thornton, J.M., 1993. PROCHECK – a program to check the stereochemical quality of protein structures. J App Cryst 26, 283–291.
Leslie, A.G.W., 1992. Recent changes to the MOSFLM package for processing film and image plate data. Joint CCP4 + ESF-EAMCB Newsletter on Protein Crystallography, No. 26.
Logue, S.E., Elgendy, M., Martin, S.J., 2009. Expression, purification and use of recombinant annexin V for the detection of apoptotic cells. Nat Protoc 4, 1383–1395.
MacKenzie, D.A., Tailford, L.E., Hemmings, A.M., Juge, N., 2009. Crystal structure of a mucus-binding protein repeat reveals an unexpected functional immunoglobulin binding activity. J Biol Chem 284, 32444–32453.
Murshudov, G.N., Vagin, A.A., Dodson, E.J., 1997. Refinement of macromolecular structures by the maximum-likelihood method. Acta Crystallogr D Biol Crystallogr 53, 240–255.
Nobbs, A.H., Lamont, R.J., Jenkinson, H.F., 2009. Streptococcus adherence and colonization. Microbiol Mol Biol Rev 73, 407–450.
Evans, P.R., 1993. Data reduction. In: Proceedings of CCP4 Study Weekend on Data Collection and Processing. Daresbury Laboratory, Warrington.
Regev-Yochay, G., Dagan, R., Raz, M., Carmeli, Y., Shainberg, B., Derazne, E., Rahav, G., Rubinstein, E., 2004. Association between carriage of *Streptococcus pneumoniae* and *Staphylococcus aureus* in Children. JAMA 292, 716–720.
Ren, J., Wen, L., Gao, X., Jin, C., Xue, Y., Yao, X., 2009. DOG 1.0: illustrator of protein domain structures. Cell Res 19, 271–273.
Roos, S., Jonsson, H., 2002. A high-molecular-mass cell-surface protein from *Lactobacillus reuteri* 1063 adheres to mucus components. Microbiology 148, 433–442.
Rucker, A.L., Pager, C.T., Campbell, M.N., Qualls, J.E., Creamer, T.P., 2003. Host-guest scale of left-handed polyproline II helix formation. Proteins 53, 68–75.
Sheldrick, G.M., 2008. A short history of SHELX. Acta Crystallogr A 64, 112–122.
Taroni, C., Jones, S., Thornton, J.M., 2000. Analysis and prediction of carbohydrate binding sites. Protein Eng 13, 89–98.
Williamson, M.P., 1994. The structure and function of proline-rich regions in proteins. Biochem J 297 (Pt 2), 249–260.